LAWRENCE
LIVERMORE
NATIONAL
LABORATORY

LLNL-CONF-673959

Implementation of an Enhanced Permanently-Installed, Neutron Activation Diagnostic Hardware for the National Ignition Facility

D. Jedlovec, E. Edwards, J. Carrera, C. Yeamans

July 7, 2015

SPIE Optics and Photonics 2015
San Diego, CA, United States
August 9, 2015 through August 13, 2015

Disclaimer

Implementation of an Enhanced, Permanently-Installed, Neutron Activation Diagnostic Hardware for NIF

Donald R. Jedlovec, Ellen R. Edwards, Jorge A. Carrera, and Charles B. Yeamans
Lawrence Livermore National Laboratory, 7000 East Avenue, Livermore, CA USA 94551-0808

ABSTRACT

Neutron activation diagnostics are commonly employed as baseline neutron yield and relative spatial flux measurement instruments. Much insight into implosion performance has been gained by deployment of up to 19 identical activation diagnostic samples distributed around the target chamber at unique angular locations. Their relative simplicity and traceability provide neutron facilities with a diagnostic platform that is easy to implement and verify. However, the current National Ignition Facility (NIF) implementation relies on removable activation samples, creating a 1-2 week data turn-around time and considerable labor costs. The system described here utilizes a commercially-available lanthanum bromide (cerium-doped) scintillator with an integrated MCA emulator as the counting system and a machined zirconium-702 cap as the activation medium. The device is installed within the target bay and monitored remotely. Additionally, this system allows the placement of any activation medium tailored to the specific measurement needs. We discuss the design and function of a stand-alone and permanently installed neutron activation detector unit to measure the yield and average energy of a nominal 14 MeV neutron source with a pulse length less than one nanosecond.

Keywords: neutron activation, NIF, lanthanum bromide

1. INTRODUCTION AND MOTIVATION

Permanently installed activation detectors have long been identified as an area of potential performance improvement for the neutron activation diagnostic system. Remotely-operated detectors installed in the target bay can measure shorter-lived isotopes, provide rapid results at reduced cost and overhead, and may open up new capabilities.

Presently, NIF neutron yields are measured by a suite of neutron activation diagnostics (NAD) utilizing the activation and subsequent counting of target material placed in and/or around the NIF target chamber. The ^{115}In(n,n') $^{115\text{-m}}$In reaction measures D(D,n) neutron yield and both ^{90}Zr(n,2n)^{89}Zr and ^{63}Cu(n,2n)^{62}Cu are used for D(T,n) yield measurements. Activation diagnostics are considered one of the primary neutron yield measurements because they produce results independent of any other diagnostic system. Measurements from other diagnostics are calibrated to activation results.

The current Flange-NAD system measures absolute neutron yield, and also the relative spatial distribution of unscattered primary neutrons leaving the fusion capsule assembly through the ^{90}Zr(n,2n)^{89}Zr reaction at 19 locations (Figure 1).

A significant limitation of the current implementation is the relative sensitivity of the ^{90}Zr(n,2n)^{89}Zr and ^{63}Cu(n,2n)^{62}Cu reactions to both core velocity and differential scattering, leading to difficulty in mapping activation at the target chamber wall to fuel geometry. Additionally, the reliance on removable activation samples leads to a fundamental lower limit on the half-life of the activated product. The NIF neutron diagnostic capability would be greatly improved by developing a NAD system utilizing an activation medium with more advantageous nuclear properties and a detector system integrated with the activation medium and installed on or near the target chamber.

Pursuant to this, we are developing a prototype Neutron Isomeric Ratio Detector (NIRD) that is based on installing detectors at existing zirconium activation locations and measuring the isomeric ratio of ^{89}Zr/$^{89\text{m}}$Zr through the relative intensities of the 909 keV and 588 keV gamma rays (Figure 2). The ^{90}Zr(n,2n) reaction populates $^{89\text{m}}$Zr in an isomeric ratio that changes significantly over the 13-15 MeV region of interest for DT fusion neutron diagnostics. By measuring the ^{89}Zr/$^{89\text{m}}$Zr activity ratio as well as the ^{89}Zr activity, the neutron energy can be deconvolved from the number of neutrons.[1]

2. PROJECT SCOPE

The first project milestone is to demonstrate an installed activation diagnostic capable of quantifying the 909 keV photopeak resulting from the decay of ^{89}Zr (3.27d half-life). Such a diagnostic, when deployed throughout the NIF target chamber, can replace the exiting removable activation samples, providing data in less time and at considerable cost savings. Our stretch goal is to resolve the 588 keV photopeak resulting from the decay of ^{89m}Zr (4.1m half-life), which allow the determination of the ^{89}Zr/^{89m}Zr activity ratio important for neutron spectrometry.

Phase 0 Prototype design and proof of concept – **COMPLETE**

Phase 1 Prototype testing at NIF – **TO COMPLETE September 2015**

Install detector in target bay using existing network cable runs

Setup manual shot trigger to detector

Operational qualification on numerous DT shots

Identify and quantify ^{89m}Zr and ^{89}Zr production by measurement of 588 keV and 909 keV photopeaks

Phase 2 Integrate a single prototype detector with the full NIF IT system – **CALENDER 2016**

Interface detector to NIF integrated computer control system

For a DT shot, measure and report yield 5-10 minutes post-shot, measure isomer ratio

Performance qualification

Phase 3 NIF Operation and expansion to many of the 19 flange NAD locations – **CALENDAR 2017**

3. DESIGN DESCRIPTION

Ultimately, NIRD units are intended to replace the passive neutron activation diagnostic locations shown in Figure 1. For the prototype NIRDs we have mounted $LaBr_3$(Ce) detectors on tripod supports. The detector is usually mounted on or in close proximity to a flange on the NIF target chamber. The detector is an integrated package containing a multi-channel analyzer, with a single connection for power and signal over Ethernet. We use a Power-over-Ethernet injector (PoE) for long line operation, with a network-attached remote power switch to control the detector power from the NIF control room. In the control room the detector interfaces to a laptop running MAESTRO® Multichannel Analyzer Application Software. A typical setup at the NIF target chamber is shown in Figure 3.

The crystal end of the $LaBr_3$(Ce) is covered by the Target Activation Medium (TAM), which is zirconium in the prototype. The TAM geometry chosen is that of an "inverse well" detector, so the zirconium takes the form of a cap over the LaBr crystal, called here the Standard Cap TAM. The multi-channel analyzer is encased in a low density polyethylene sleeve. Refer to Figures 4 and 5. Figure 6 shows the detector assembly on tripod mount in a typical position on NIF target chamber.

We found the performance of the detector to be influenced by the electro-magnetic pulse associated with the shot and also by high count rates from nearby materials activated by direct and scattered neutrons. For this reason we tested the detector in several configurations. Figure 7 summarizes these configurations.

The Standard Cap TAM configuration (Figure 8) places the unit in front of an aluminum diagnostic port cover directly in the unshielded neutron beamline. We deployed the Standard Cap configuration in two locations as shown in Figure 9. Here the TAM and LaBr Crystal are unshielded while the detector electronics are shielded by the gunite surrounding the target chamber.

The Shielded Cap configuration (Figure 6) moves the full assembly out of the port alignment position sitting behind the gunite shielding that lines the outside of the target chamber.

The Shielded Remote configuration (Figure 10) eliminates the use of the TAM and replaces it with a 70mm diameter by 15mm thick Neutron Activation Disk (NAD). In this configuration the detector remains shielded behind the gunite while the NAD is mounted on the diagnostic port cover, in the unshielded neutron beamline.

The Translatable Cap configuration (Figure 7) has the detector assembly sitting behind the gunite shielding and the TAM sitting in front of the diagnostic port cover during the event. After the primary neutrons have passed, activating the cap, the detector moves into position mating with the TAM. This minimizes the activation of the $LaBr_3(Ce)$ crystal itself while maximizing the activation of the TAM.

Generally, our best results are obtained with the Standard Cap TAM configuration. This provides the highest activation signal since the activation medium is in the direct neutron beam, with the detector electronics shielded by the gunite. However none of these configurations will allow us to resolve both the 588 keV and 909 keV photopeaks for both low and high yield NIF shots. For high yield shots we can only resolve the 909 keV (3.2d half-life) photopeak. Here the background caused by activation of the target chamber components and also by activation of the $LaBr_3(Ce)$ detector itself swamps the 588keV photopeak. By the time this background has decayed away the 588 keV (4.2m half-life) is gone as well. For low yield shots, there may not be enough activity to resolve the 909 keV photopeak, although the 588 keV peak is easily resolved. What this means for NIF is that the Zirconium NIRD can replace the existing, removable NADs, but we have yet to demonstrate measurement of the $^{89}Zr/^{89m}Zr$ activity ratio.

The unique environment in the NIF target bay required a trial and error approach for offloading the detector data. The initial implementation used a local laptop and Power over Ethernet (PoE). This worked well for low energy experiments or in heavily shielded locations, but for unshielded or high energy events the laptop would reset promptly after the event. To isolate the laptop we used the NIF closed network to connect a secured laptop from the control room to the detector's digiBASE-E Ethernet port. Networking the counting hardware did allow the detector to run during the high energy events, but prompt pulse would interrupt the Crystal + Photomultiplier Tube (PMT) to Multi-Channel Analyzer (MCA) interface. Several EMI shielding methods were explored: wire braid covers for power cables, double shielded CAT7 Ethernet cables, and copper enclosures for the detector and PoE. While the shielding does aid in protecting the Prototype Assembly from damage due to EMI, it did not solve the issue of the connection interrupt. As a result, a network-attached remote power switch was put in place to interrupt power to the detector until immediately after the high energy events.

The first $LaBr_3(Ce)$ detector, as of June 1st 2015, has been fielded on fifteen high neutron yield ($> 10^{14}$ 14 MeV neutrons) experiments and over 80 low/no yield experiments with no noticeable signs of performance degradation; low or no yield experiments can still produce a strong EMI/EMP, however. Six months after the original detector was installed in the NIF target bay a second $LaBr_3(Ce)$ detector was deployed. The second detector is a step towards spatial analysis as well as expediting the investigation into failure modes of the $LaBr_3(Ce)$ which will aid in refining the final design of the Permanent Hardware configuration.

Table 1 - Parts List for neutron activation diagnostic prototype

Part	Manufacturer	Part Number	Description
1	Saint Gobain Crystal	LABR-1.5X1.5 LaBr3(Ce)	Scintillation detector, 1.5x1.5-in. Crystal with 2in diameter 14-pin PMT, Resolution @ 662 keV :2.6% & 2.8% (Cs137- 662keV)
2	ORTEC	digiBASE-E-CH	High Performance 14-pin PMT Base for Scintillation Detectors. Digital MCA, Preamplifier, High Voltage Supply, PoE Ethernet Connection.
3	Dataprobe Inc.	iBoot-Hub	10/100 Ethernet network attached, IP addressed, Network Controlled power switch

4. DATA PROCESSING AND ANALYSIS TECHNIQUES

Extraction of photo peaks in the presence of a high (activation) background of nearby components

The detector is turned on after the shot to avoid the prompt signal and EMI interference. MAESTRO® Version 7 is used to collect the data in list mode. In list mode the time and energy (channel) is recorded with each detected event. The data is stored in a binary .Lis file, which is then processed with MATLAB® to extract a list of timestamps and channels.

All of the analysis is done in MATLAB®. Histograms are made by post-processing in which events are integrated in each channel over a specified time window. The advantage of using list mode is the time bin can be changed depending on the half-life of the isotope of interest. To analyze the ^{89m}Zr peak (half-life 4.16 minutes, 588 keV), a time bin of 1 or 2 minutes is used. This is short enough to see the decay but long enough for good statistics. The histograms for each time bin are then stacked next to each other to display the time evolution of the spectrum. Figure 11 is an example. Figure 12 is a plot of one time bin from Figure 11.

The next task is to determine the decay of each peak. To identify the energy range of interest, a histogram of a single time bin is used (e.g. Figure 12). The minimum and maximum energies in the peak are selected, along with the number of channels on each side to use for background subtraction. The number of background channels is chosen based on nearby peaks, so nearly overlapping peaks might only have a few points between them for background subtraction. Then a line is fitted to the background subtraction points, it is subtracted, and the remaining points are fit to a Gaussian distribution. The area of the Gaussian is calculated and the process is repeated for each time bin. The areas are plotted as a function of time and an exponential curve fit with the known half-life is applied. Using the energy and half-life, it is possible to identify what isotopes are present. When the isotope is known, the measured count rate can be extrapolated to shot time to determine the initial count rate. When the system is calibrated with an empirical constant to account for all neutron transport and detector response efficiencies, the initial count rate can be converted to yield. An example is shown in Figure 13.

5. RESULTS

The results of three different scenarios are shown in Figures 11, 14, and 15.

For Figure 14 the detector was located 20 m from target chamber center. The background is much lower when the detector is far from the target, and it is possible to see individual peaks near the beginning of the shot.

Figure 11 is for a low yield shot with the detector at the target chamber, 5m from target chamber center (Standard Cap configuration as shown in Figure 8). Here, the peak from ^{89m}Zr is visible and quantifiable.

For yields of ~10^{15} neutrons the activation background signal is so high it covers up the ^{89m}Zr signal (see, for example, Figure 15). Even if this problem is never solved, the ground state Zr peak is still visible because it decays slowly ($t_{1/2}$=78.41 hr) compared to the background (refer to Figure 16), and the detector has time to fully recover.

Using the detector setup we demonstrated the ability to identify unknown isotopes based on energy and half-life. Figure 14 has a short-lived peak around 207 keV, which also appears in low-yield shots (Figure 11). By fitting the peak's exponential decay the half-life was 5.25+/-0.17 s. Using this information, the peak was determined to be a metastable state of ^{79}Br, that occurs when neutrons scatter inelastically off the ground state. ^{79}Br is 51% of natural Br, which is part of the detector.

Both the ^{89m}Zr and ^{89}Zr peaks have been observed with the detector in the target bay, and verified by using the half-life of the peak decay. The next steps are to compare the NIRD detector with the existing system to calibrate the efficiency, and to determine the optimal configuration in the target bay to reduce the prompt background signal.

6. CONCLUSION

Permanently installed activation detectors have long been identified as an area of potential performance improvement for the neutron activation diagnostic system. We have demonstrated a prototype neutron activation detector that can replace all nineteen removable activation media on the NIF target chamber exterior. Future work will focus on reducing the background signal just after shot time. This will allow us to measure the isomeric ratio of ^{89}Zr/^{89m}Zr that can be used to calculate the neutron spectrum.

7. ACKNOWLEDGEMENTS

This work was performed under the auspices of the U.S. Department of Energy by Lawrence Livermore National Laboratory under Contract DE-AC52-07NA27344.

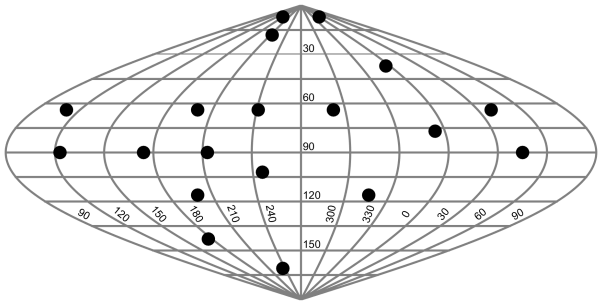

Figure 1. NIF Flange NAD deployment on NIF Target Chamber as of July, 2015

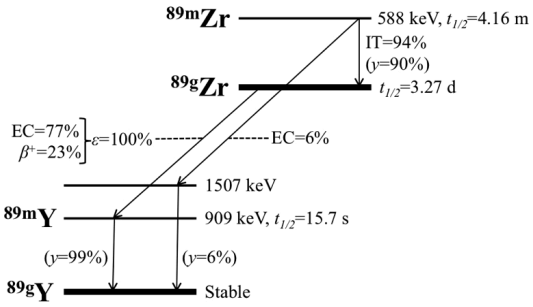

Figure 2. Simplified decay scheme

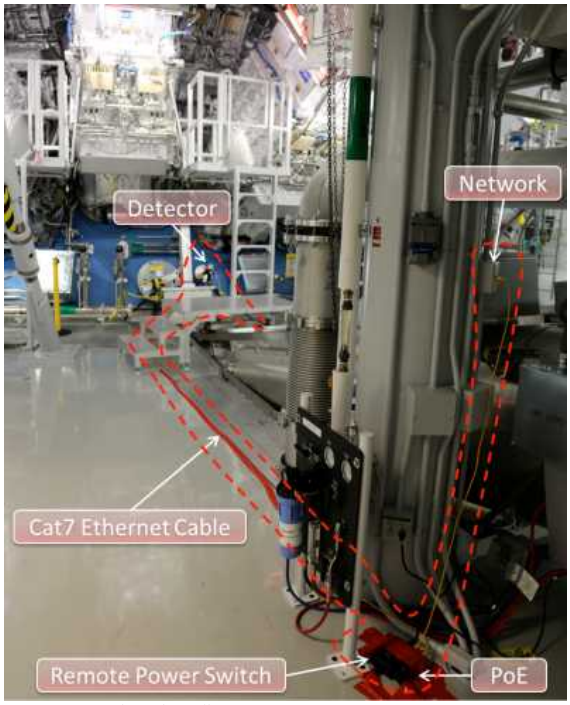

Figure 3. Typical detector setup at Target Chamber flange

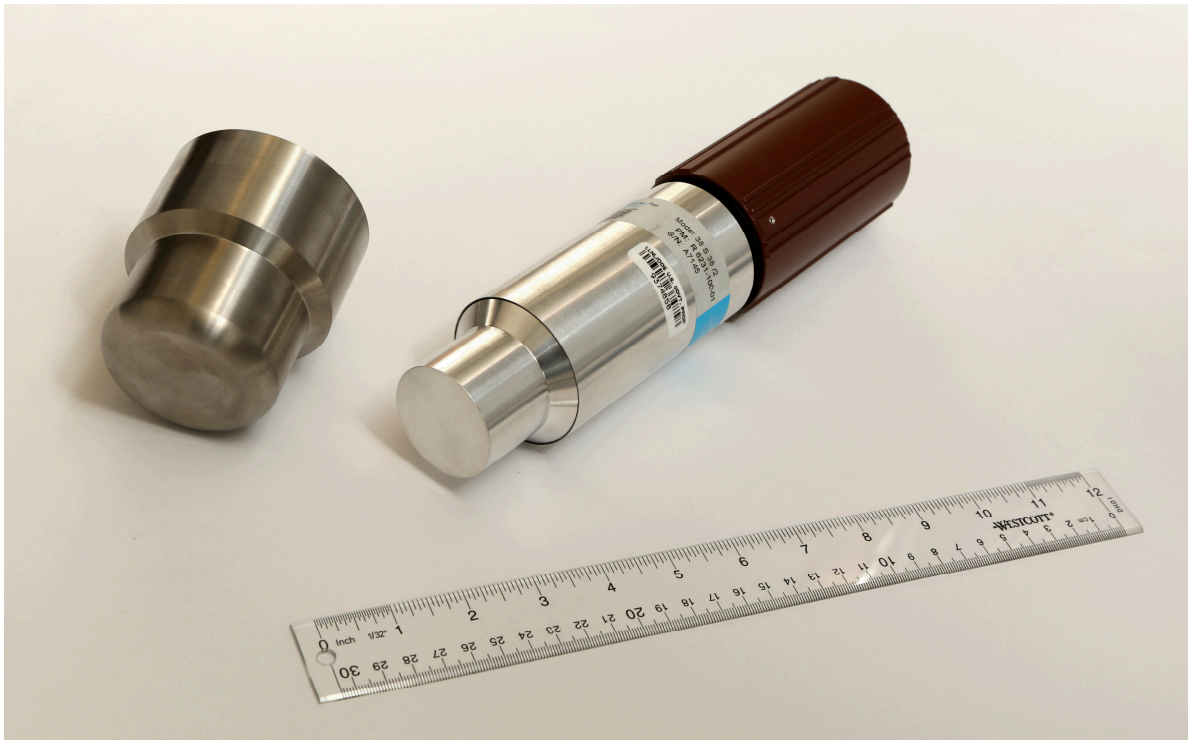

Figure 4. The Activation Material Cap fits over the crystal end of the detector

Figure 5. Low density polyethylene protective cover and shield

Figure 6. Detector assembly on tripod mount in typical position (shielded Cap configuration) on NIF target chamber

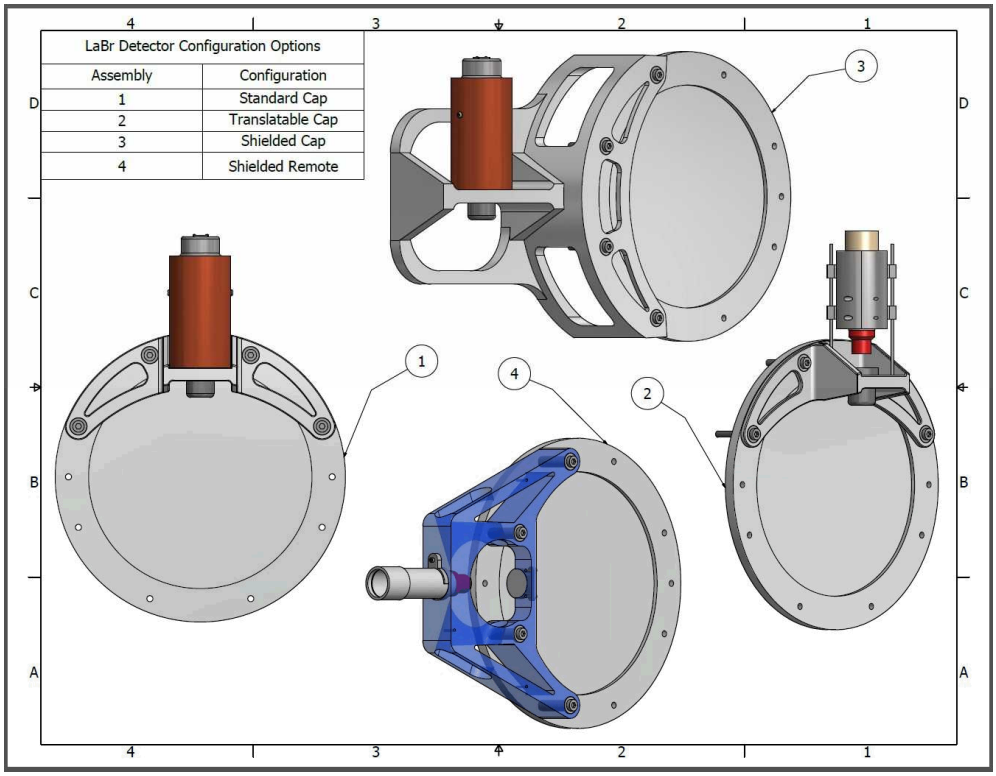

Figure 7. Detector assembly configuration concepts

Figure 8. Typical standard cap TAM configuration

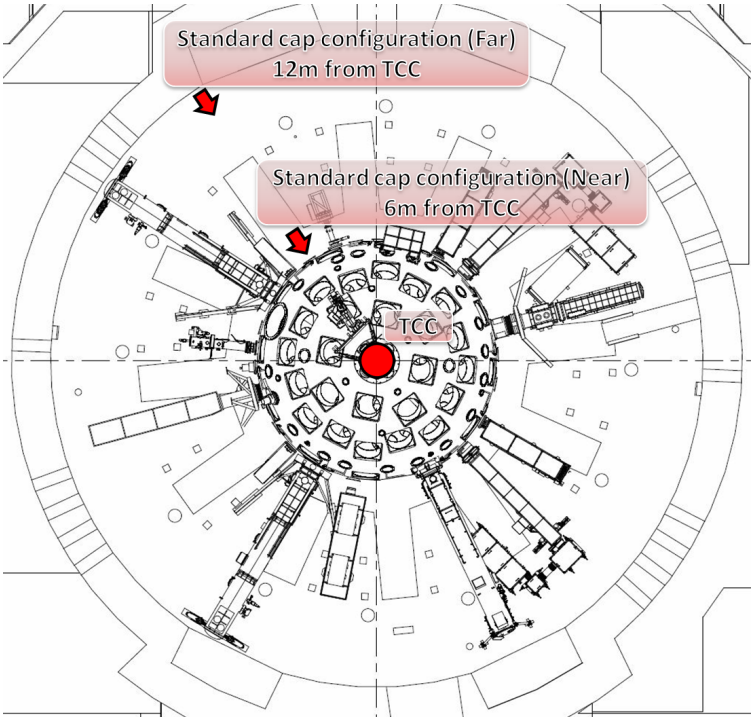

Figure 9. Detector location in the Target Bay, Standard Cap configuration

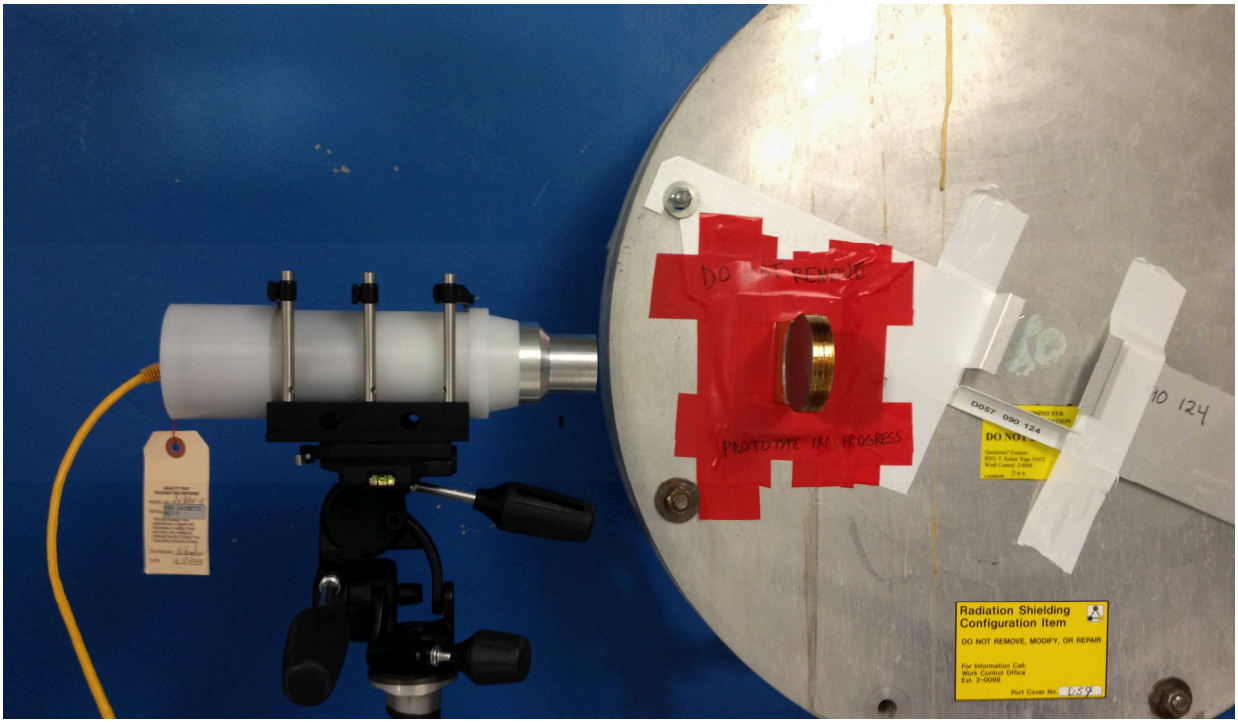

Figure 10. Shielded Remote configuration

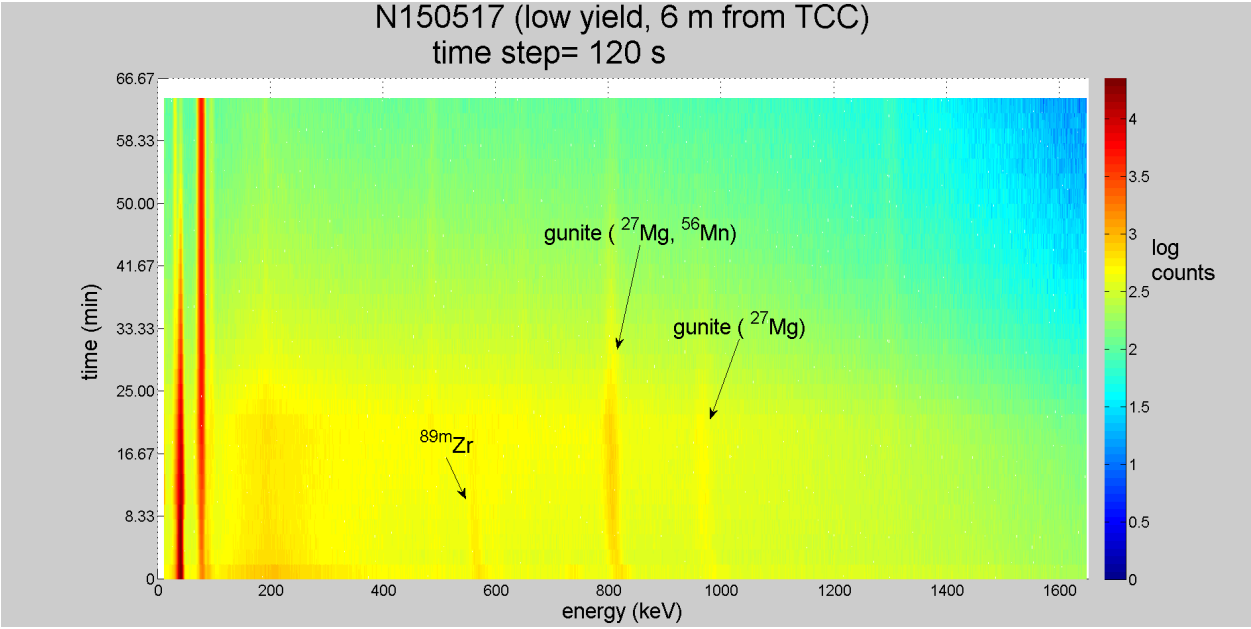

Figure 11. A time-resolved graph created by combining many histograms. The colors are on a log scale. Standard cap.

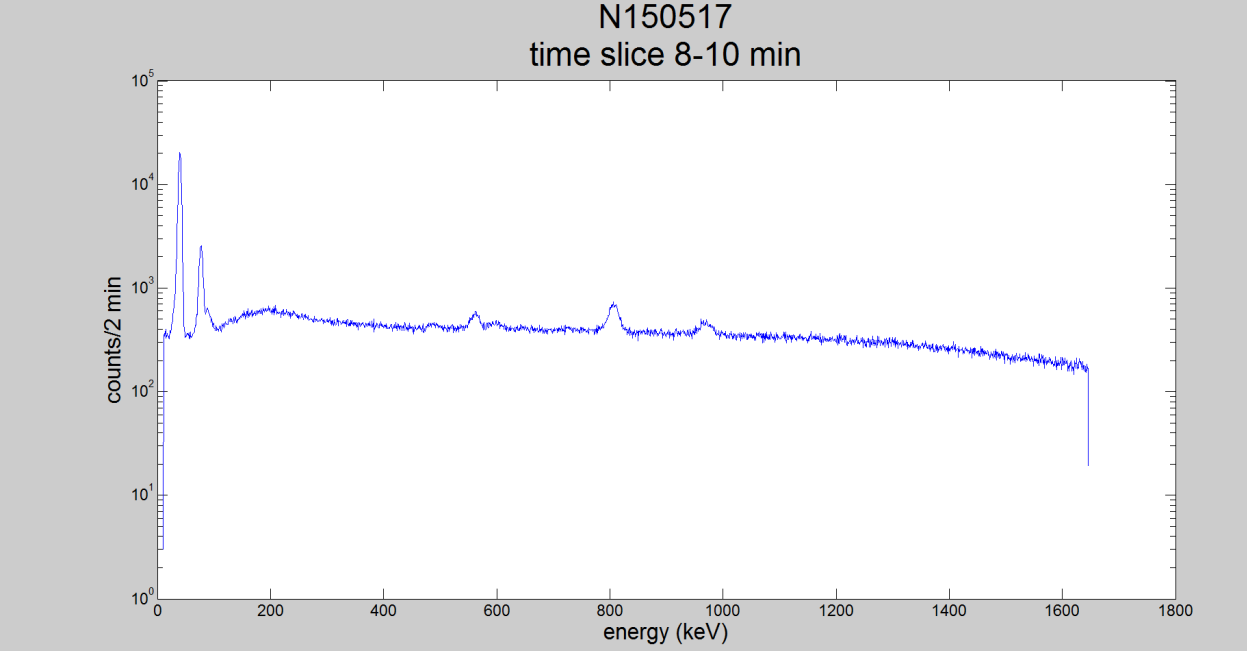

Figure 12. One of the 2-minute histograms making up Figure 11. These histograms are used to find the energy cutoffs of each peak. Standard cap.

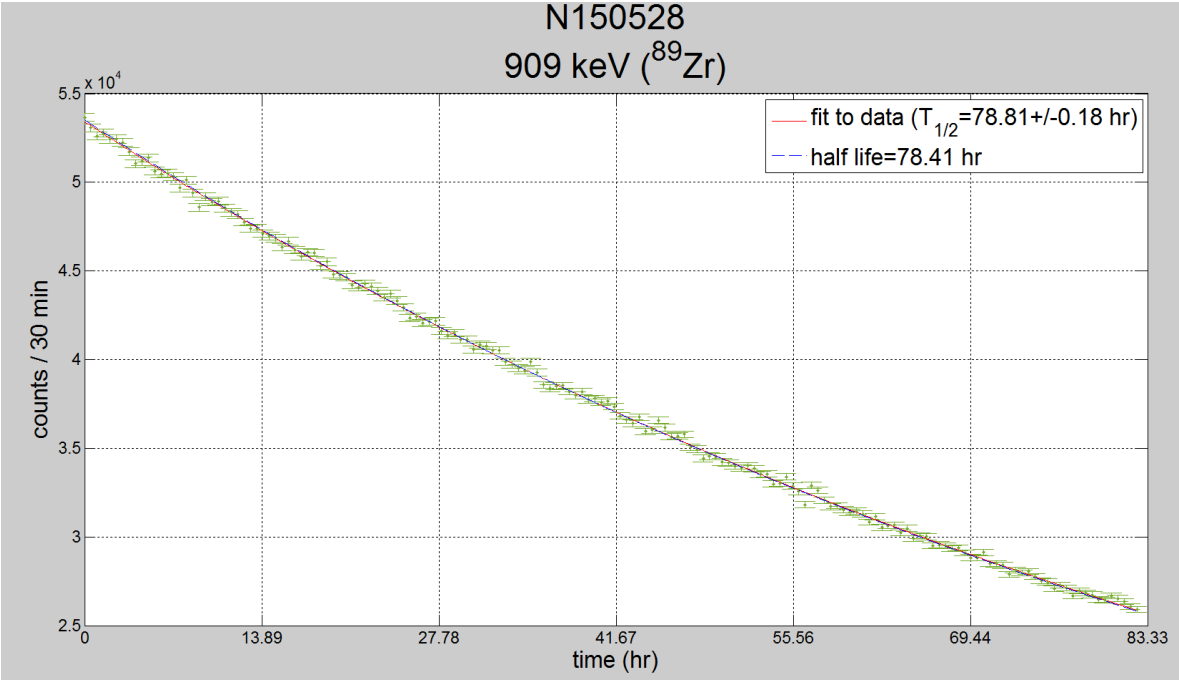

Figure 13. This Figure uses the data from Figure 16. The decay of the 909 keV photopeak identifies it as ^{89}Zr. When the system is calibrated the neutron yield will be found by extrapolating to shot time.

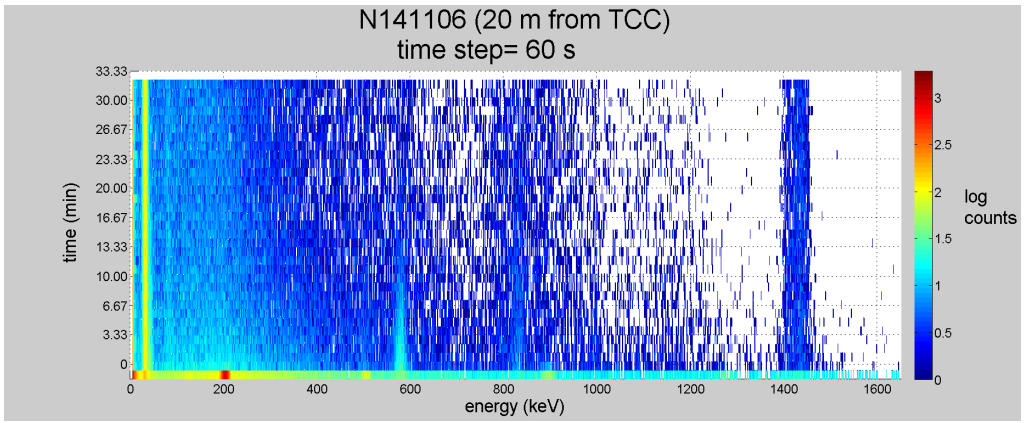

Figure 14. The detector was far enough away that it did not turn off at the beginning of the shot. Here we can see the 588 keV photopeak but not the 909 keV

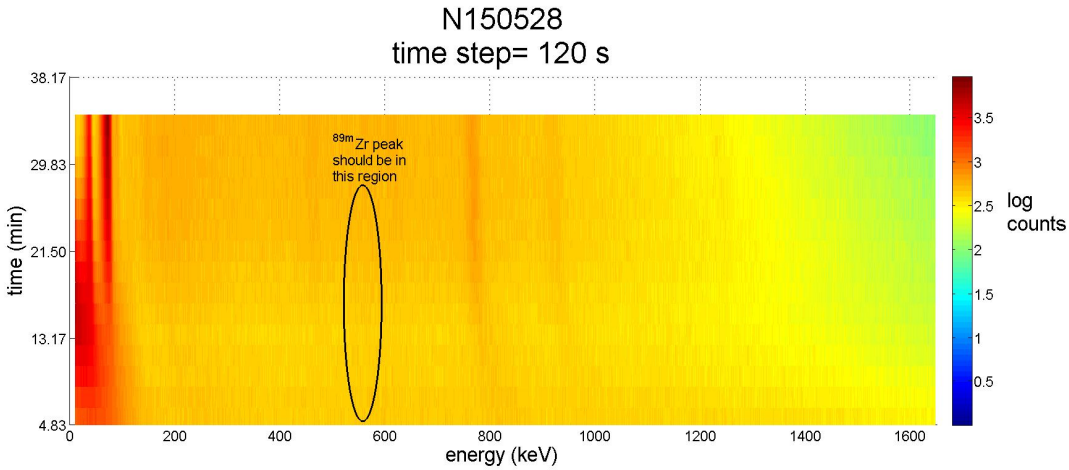

Figure 15. A high neutron flux overloads the detector. It takes time to recover but the ^{89m}Zr has decayed by this time. Shielded cap.

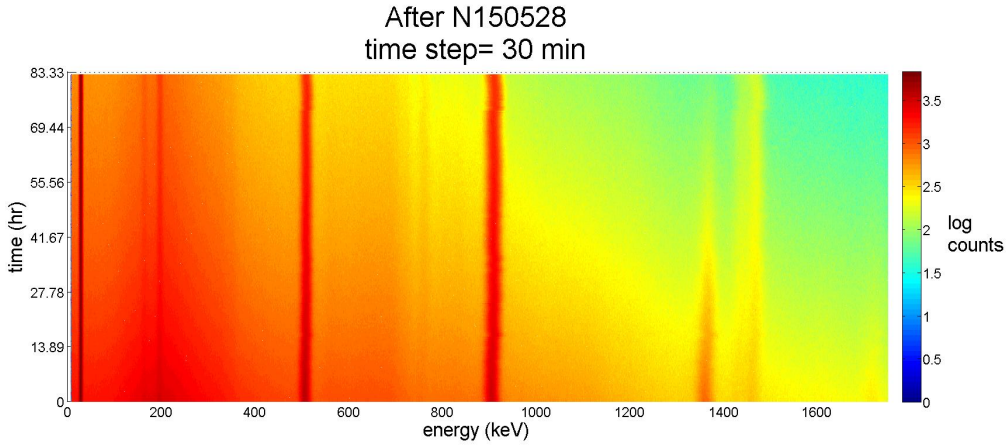

Figure 16. The same shot as Figure 16, but using a larger integration time to focus on ^{89}Zr (78.41 hour half-life, 909 keV). The detector has enough time to recover and record the ^{89}Zr ground state. Shielded cap. Yield = 6e15 neutrons.

REFERENCES

[1] Yeamans, C. B., Bleuel, D. L., and Bernstein, L. A. "Enhanced NIF Neutron Activation Diagnostics" Rev. Sci. Instrum. **83**, 10D315 (2012); doi: 1063/1.4739230.